Impressive Reduction of Dark Current in InSb Infrared Photodetector to achieve High Temperature Performance

Saman Salimpour[1], Hassan Rasooli Saghai[*,1]

[1] Department of Electrical Engineering, Tabriz Branch, Islamic Azad University, Tabriz, Iran.

Abstract: Infrared photo detectors have vast and promising applications in military, industrial and other fields. In this paper, we present a method for improving the performance of an infrared photodetector based on an InSb substance. To achieve good performance at high temperatures, thermal noise and intrusive currents should be reduced. For this purpose, a five-layer hetero structure photodetector based on We introduce n+ InSb / n+ $In_{1-x}Al_xSb$ / π InSb / p+ $In_{1-x}Ga_xSb$ / p+ InSb to improve the thermal performance in the mid-wavelength infrared (MWIR) range. With inserting of two thin layers from InAlSb and InGaSb on both side of the new (π) optical absorber created a barrier in the structure that prevents from entrance of diffusion currents and noise carriers at n+ and p+ regions into the active area. And also by reducing the density of unwanted carriers in the active layer, leads to decrease dark current, which is the main limiting factor for photodetectors' performance based on InSb. Our proposed design reduced 49% dark current, increased 57% resistivity (R0) and increased 39% detectivity at 300K. Simulation of the structure was done using the SILVACO ATLAS software.

Keyword: InSb Infrared Photodetector, High Temperature, Dark Current, Detectivity, Hetero Structure.

1. INTRODUCTION

Infrared photodetector based Narrow bandgap semiconductor material of mid-wavelength are widely used for civilian and military applications such as proximity detection, thermal imaging cameras, remote sensing, quantum information technology, astronomy systems, molecular "fingerprint" imaging, micro-Hall sensors, free space telecommunication, optical radar, missile guidance, scientific research, and so on. Also, these kinds of high-performance photodetectors have been made over the past five decades [1, 2, 3, 6, 8, 9, 13]. The first triple-five (III-V) semiconductor material used for mid-wavelength infrared (MWIR) photodetector was InSb [34, 35, 10]. The InSb material has a direct bandgap and narrow-band energy (Eg= 0.17ev), and is considered as a

---

* Corresponding author. Email: **h_rasooli@iaut.ac.ir**

group of triple-five semiconductor materials. InSb is one of the materials commonly used in infrared detectors due to its narrow bandgap, InSb in particular has substantial potential due to its sensitivity spans in optical wavelengths from 1.5 to 7μm at room temperature. [13, 14, 5, 8]. InSb has more benefits than HgCdTe, such as easy homogeneous growth and stronger covalent bonding, and is one of the infrared materials used in a wide range [24]. The InSb substance is more complete than HgCdTe, and for InSb, the field of quality is appropriately provided [25]. The infrared guidance and infrared imaging systems that are made by narrow band gangs are commonly used. Detectors require cooling systems to obtain the highest sensitivity in the mid-wavelengths (3 to 5 μm) and high (8 to12 μm) of the electromagnetic spectrum [26,30]. It has also been assumed previously that access to optimal properties of narrow band semiconductor materials is only possible at cool temperatures, due to the fact that at high temperatures noise is predominant in the system and this is a bad parameter for the system. The use of cooling systems also adds cost, power consumption, and weight to infrared detectors [27, 28, 33]. Hence, the acquisition of infrared systems with high temperature performance has attracted a lot of attention. One of the promising methods to achieve this was first suggested by Ashley et al. [24, 32]. The method presented by them was based on the minority-carrier extraction and exclusion technique. Special considerations should be given to designing detectors based on narrow band gaps. In this case, various mechanisms such as tunneling, surface recombination, Auger and radiative should be investigated. Scientific research should also be carried out to improve the quality and efficiency of devices in the field of quantum efficiency, responsivity and detectivity. The use of hetero structure for designing detectors can significantly improve their performance. In a double hetero structure, a substance with a small band gap is placed between two materials with a large band gap. Incompatible structures are used to prevent the arrival of carriers into active region [21,29-31,34]. In this paper, a five-layer photodetector is provided based on InSb-related materials for high-performance and mid-wavelength infrared (MWIR) functions. The results obtained from our simulation are compared with the diagram obtained by M. Nadimi and A.sadr [19, 23].

2. DEVICE STRUCTURE AND SIMULATION

Narrow band gap semiconductors have several characteristics. These properties are due to their energy band structure. Including these materials, InSb has specific electronic features, such as low electron mass, high electron mobility (77000 cm^2 V^{-1} s^{-1}), high saturation velocity, and has large Bohr radius (~ 60 nm) and is an attractive material for high speed electronics and infrared optoelectronics [11]. It also has significant optical parameters, such as a small direct bandgap, a high ratio of stimulated emission to spontaneous emission and a large nonlinear

capability [22]. Narrow band gap semiconductors operate at high temperatures as conductive materials, and the temperature of these devices should be reduced to 77K by cooling systems to achieve optimal performance. The presence of these cooling systems limits the use of detectors in portable devices. This suggests that the development of MWIR optical detectors that are capable of operating at high temperatures is essential [29]. The schematic structure of Fig.1 (a) and (b) shows, respectively, the three-layer and four- layer photodetectors designed by the previous author, respectively.

In Fig. 1a, a three-layer photodiode of the n+-π-p+ conjugate structure is represented by a non-equilibrium mode with the application of an electric field. In this structure, the πp region is an exclusion contact, which does not cause any blockage to the majority carrier, but prevents the infiltration of minority carriers, and the πn region is an extraction contact, which causes It will be possible to limit the Auger mechanism by extracting minority carriers. The structure of the three layers' n+-π-p+, using the minority-carrier extraction and exclusion technique, limited the noise generated by the Auger mechanism, so the detector function was possible at a temperature of 200k [26].

In Fig. 1b, a four-layer photodetector shows an inconsistent structure n+-π-p+-p+. The performance of InSb-based infrared photodetector at high temperature was limited by thermal noise. The use of an imbalance model based on the technique of extraction and removal of minority carriers was proposed to increase the performance of this device. These methods are used to reduce the electron density and hole. The extraction technique involves a low amount of impurities in the active region (π), in which infrared rays are absorbed, and the presence of high impurities on the sides of the active region leads to the formation of a three-layer n+-π-p+ structure. In order to reduce the penetration currents from the p+ region, they placed a thin layer of large bandgap material between the areas π and p+. This led to the formation of a four-layer structure n+-π-p+-p+. The results indicate that the placement of high bandgap material between the π and p+ layers reduces the dark current of the detector. This caused the detector to operate at a temperature of 220K with $\lambda = 4\mu m$ and Detectivity = $4.87 \times 10^9 cmHz^{1/2}/w$ [23].
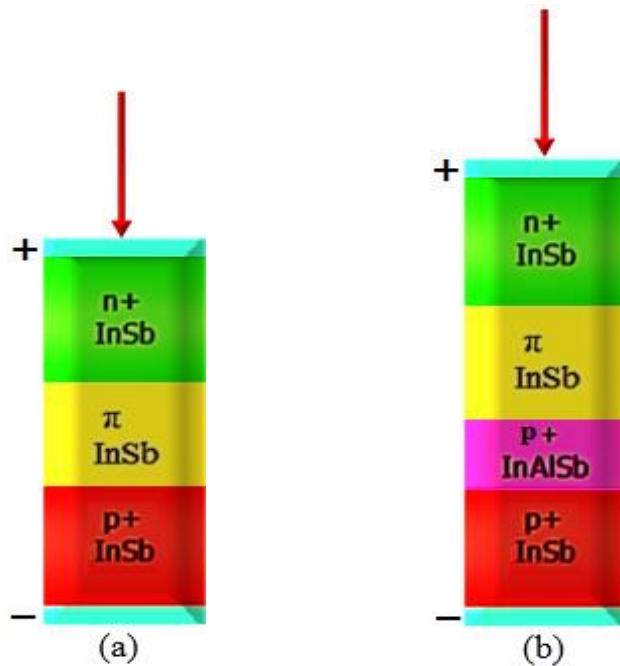
Fig.1: Schematic structure (a) three-layer homostructure, (b) four-layer heterostructure

One of the important mechanisms in detectors is the penetration flow, which has a detectable amount of absorption in the outer parts of the active region. This effect is reduced in regions with high impurity by recombination phenomenon. Infiltration carriers in the discharged area provide an opportunity to disperse in the active layer. Fig. 2 shows the infiltration flows of the carriers.
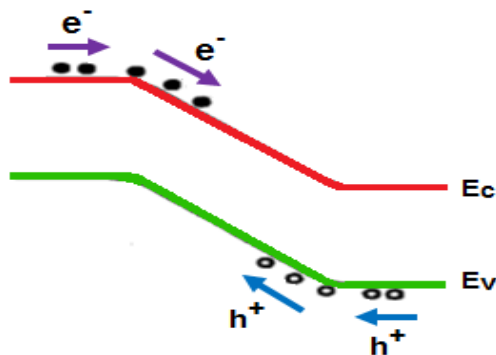
Fig.2: The origins of diffusion current

The current of electron and cavity penetration at the edge of the discharge zone is obtained by the following relations [15]:

$$J_e = qD_e \frac{\partial n}{\partial x} = qD_e \frac{\Delta n}{L_e} \tag{1}$$

$$J_h == -qD_h \frac{\partial p}{\partial x} = qD_h \frac{\Delta p}{L_h} \tag{2}$$

Here, D_e (D_h) and L_e (L_h) are diffusion coefficients and diffusion lengths for electrons (holes), respectively. For detectors, the design of the Hetero structure restricts the entry of intrusive carriers to the active layer, causing radiation to be absorbed in the intrinsic region, in which the field is large [24]. The schematic structure Fig.3 shows a five-layer photodetector that is presented in this paper, and the results of its output parameters are compared with previous structures. The shapes of our detector n+ InSb/n+ $In_{1-x}Al_xSb/\pi$ InSb/p+ $In_{1-x}Ga_xSb$/p+ InSb, designed to prevent the entry of intruder carriers into the active region, and minimize the amount of intrusive current in the structure.

Fig.3: Schematic structure of the five-layer heterostructure

Because of the difference in the density of electrons and holes in semiconductors of type n and type p, the electrons tend to enter the region of p from the n region, and also the holes want to enter the area p into the n region [25]. Intrusive current is the basic mechanism in photodetectors, which are

generated by the movement of minority carriers from the region p to the n region [29]. For the device to perform at higher temperatures, the produced heat carriers should be brought to the lowest level [4]. The heterogeneous structures handle substrates for achieving high-performance devices [25]. In a double hetero structure, it is prevented from entering carriers to the active region, because the active region has a small bandgap that lies between two region with a large bandgap, and this banding gap creates dams. The potential is in the structure. Therefore, the infiltration of the carriers into the active region is severely restricted [26]. Dark current mechanism is the most important problems of narrow–energy gap semiconductor material based MWIR photodetectors. The application of the barrier layer on the infrared photodetector based InSb semiconductor material effectively decreased their dark currents and increased their operating temperatures and detectivity. Usually, dark current mechanism is attached to the generation-recombination (G-R) mechanism where the thermally generated carriers are excited from the valence band energy to the conduction band energy via the defects existing between these two bands. However, the generation- recombination mechanism has an activation energy that is half of the semiconductor energy gap[6,7,8]. In our proposed structure (Fig.3), a 25nm thin layer of $In_{1-x}Ga_xSb$, a padding type P, and a casserole x=0.8, which is a large band gap (Eg = 0.54ev) with direct band gap [27] between the areas π and p+. This layer created a barrier in a conduction band, which severely restricted the entry of the carriers of the p+ region to the active region. Also, the entry of n+ region carriers into the active region is one of the important sources of dark currents that should be prevented from transferring them to the active region [27].

To do this, we plotted a thin 25nm thin layer of $In_{1-x}Al_xSb$ with doping type n and x=0.1, which is a large band gap material, between the regions π and n+. This layer created a barrier in the valence band, which prevented the arrival of minority carriers in the n+ area into the active region. Our design, with a performance of 300k, resulted in a 49% reduction in dark current, an increase of 57% in R0 and a 39% increase in detectivity. The impurity content in the n+ region is $1\times10^{18}cm^{-3}$ and the impurity content in the p+ region is 4×10^{18} cm^{-3}, and the impurity concentration in the intrinsic region is $1\times10^{15}cm^{-3}$, and the thickness of the structure in The length of the x direction is 25μm and the thickness of the different layers along the y direction in Table-I. Beam at the intensity of $1w/cm^2$ enters the photodetector from the n region.

Table I
Layer thickness of the five layers heterostructure diodes

Layer	THICKNESS(MICROMETER)
n+	1
n+	0.025
π	5
p+	0.025
p+	1

The simulation of the detector structure is carried out in two-dimensional format by ATLAS software. The detector features were introduced into the DECKBUILD software section by programming commands. A numerical solution was performed using the Newton iteration. Carrier density and impurity were calculated by the Fermi-Dirac statistical model. The mobility assessment was performed using the CONMOB model [36]. The dark feature was examined using Optical, SRH, and Auger recombination's. The rate of different combinations is as follows [23]:

$$R_{np}^{OPT} = C_C^{OPT}\left(pn - n_i^2\right) \tag{3}$$

$$R_{SRH} = \frac{pn - n_i^2}{\left[\begin{array}{c}\tau_{po}\{n + n_i\exp(E_t/KT)\} + \\ +\tau_{no}\{p + n_i\exp(-E_t/KT)\}\end{array}\right]} \tag{4}$$

$$R_{Auger} = C_n\left(pn^2 - nn_i^2\right) + C_p\left(p^2n - pn_i^2\right) \tag{5}$$

where Cc^{OPT} is capture rate of carriers, C_n and C_p are Auger coefficients for electrons and holes respectively, n and p, are equilibrium electron and hole concentration, E_t is energy level of trap, n_i is intrinsic carrier concentration, T_{po} and T_{no} are SRH lifetime of holes and electrons respectively, R is recombination rate, K is Boltzmann constant and T is temperature [28].

3. Result and discussion

Fig.4a shows the energy band of the five-layer photodetector in equilibrium state and in Fig.4b under the reverse bias. In this diagram, the red and green lines represent the conduction band and the valence band respectively. Spike is due to the presence of high bandgap in the structure. High band gap materials cause a dam in the structure, which prevents the entry of minority carriers in the n and p regions into the active region.
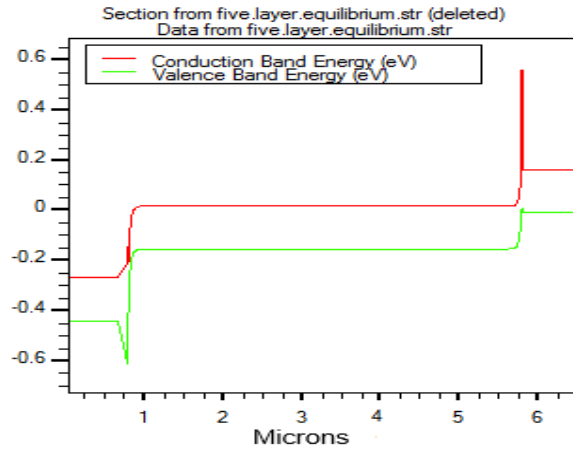
(a)
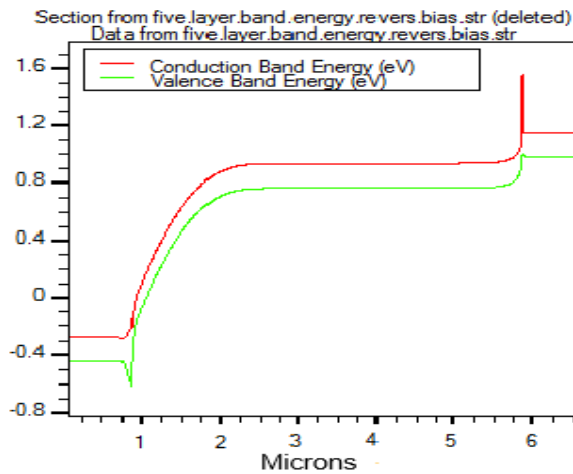
(b)

Fig.4: The energy band diagrams for five-layer heterostructure diode: (a) Equilibrium, and (b) Reverse bias

Fig.5 the current-voltage characteristic for three-layer homo structure, four-layer hetero structure and five-layer hetero structure structures at 200k, 220k and 300k, respectively. The dark current for a five-layer detector with a decrease of 49% has a value of $1/129 \times 10^{-11}$A. This indicates the ability of the five-layer structure to reduce the dark current to three-layer structure and four-layer structure [19, 23]. One of the important parameters that evaluates the function of infrared photodetector is the zero bias resistance-area (R0A), which

is determined by the dark current of the detector. The zero bias resistor is written below [23]:

$$R0 = KT/qI0 \tag{6}$$
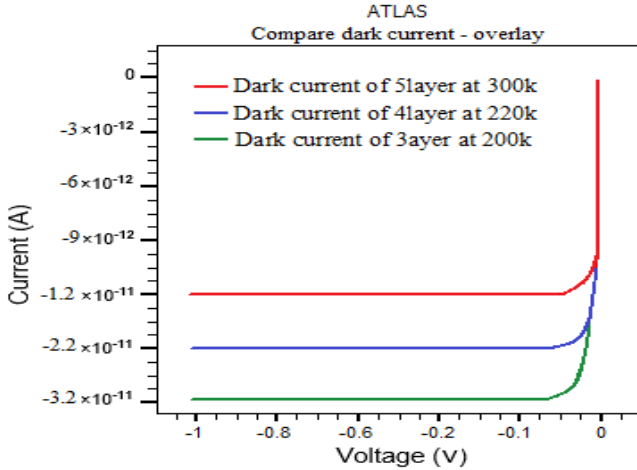
Fig.5: Variation of dark current with reverse voltage for five-layer heterostructure at 300k and four-layer heterostructure at 220k and three-layer homostructure at 200k

Figure.6 shows the variation of R0A with a temperature (T) for five-layer hetero structure, four-layer hetero structure and three-layer homo structure. As it is seen, at a lower temperature, the R0A value is increased, which indicates a decrease in dark current, also due to the reduced thermal production of the carriers [25]. In this chart, the highest value of R0A belongs to the upper curve, which is the same five-layer n+-n+-π-p+-p+ photodetector, which shows the ability of the five-layer structure to reduce the dark current of the system compared to three-layer structure and four-layer structure [19,23]. The amount of R0, reached to $1/985 \times 10^9$ Ω with 57% increase. One of the important parameters used to compare detector performance is detectivity. This parameter depends on the wavelength of incident light λ, the quantum efficiency η and the zero bias resistance-area product (R0A), and is represented by D* and its unit (cmHz$^{1/2}$/w), q is electron load, h is plank constant, c is velocity of light, and is the following is measurable [23]:

$$D* = \frac{q\eta\lambda}{hc}\sqrt{\frac{R0A}{4KT}} \tag{7}$$
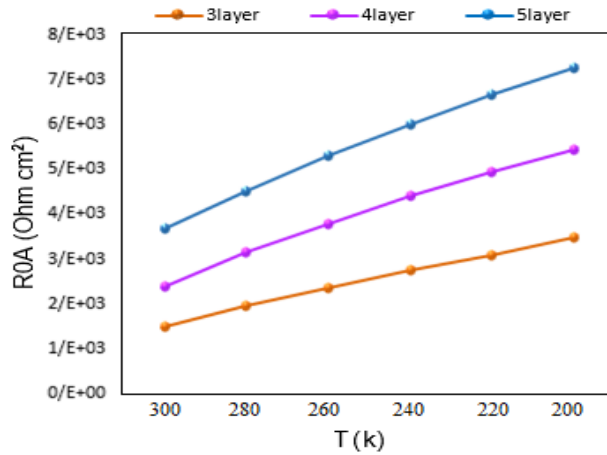
Fig.6: R0A versus T for the five-layer heterostructure and four-layer heterostructure and three-layer homostructure diodes

Fig.7 shows detectivity changes for five-layer photodetector with a wavelength of 5μm, four layers and three layers with a wavelength of 4μm at various temperatures. As it is seen, the five-layer structure has the highest amount of detectivity at different temperatures due to the inclusion of InGaSb and InAlSb in the structure, which is arranged between π-p+ and n+-π layers, respectively. This indicates the ability of the five-layer structure to increase the detectivity to three-layer structure and four-layer structure [19,23].
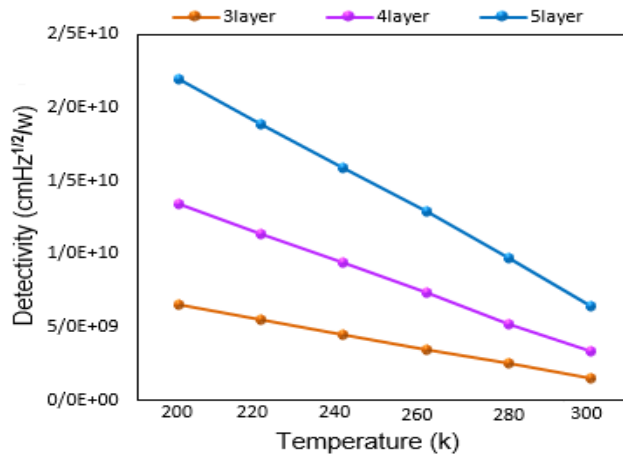
Fig.7: Variation of detectivity with temperature for the five-layer heterostructure at λ=5um and four- layer heterostructure and three-layer homostructure at λ=4um

Fig.8 shows Detectivity changes at different wavelengths for five-layer, four-layer, and three-layer photodetectors. The four-layer curve with a wavelength of 4μm and a temperature of 220k has a Detectivity value of 4.87×10^9cmHz$^{1/2}$/w. In the five-layer photodetector, with an increase in wavelength to 5μm, the precision at 300k temperature increased by 39% to 7.99×10^9 cmHz$^{1/2}$/w. This indicates the ability of the five-layer structure to increase the detectivity to three-layer structure and four-layer structure [19,23].
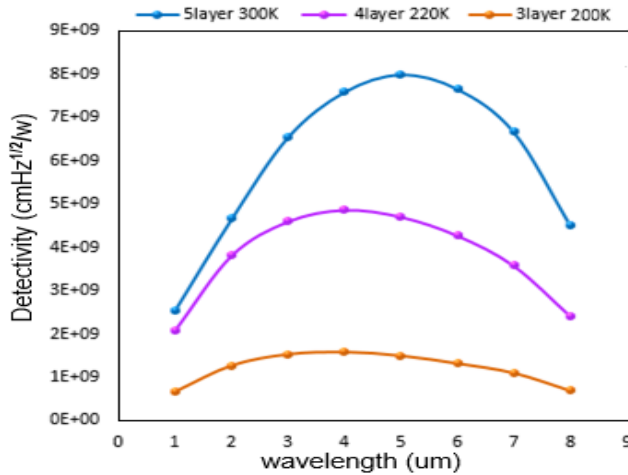
Fig.8: Variation of detectivity with operating wavelength for the five-layer heterostructure at 300k and four-layer and three-layer at 220k

Compared to Table-II, the values for increasing and decreasing dark-current parameters, zero-bias resistivity and precision for a four-layer photodetector at 220k and a five-layer photodetector at 300k are compared.

Table II
Comparison of percent increase and decrease of dark current values, zero bias resistance and detection capability, five-layer photodetector

Dark current 4layer	$2/21 \times 10^{-11}$
Dark current 5layer	$1/12 \times 10^{-11}$
% reduction of dark current at 5layer	49%
R0 4layer	$8/54 \times 10^8$
R0 5layer	$1/98 \times 10^9$

% increasing of R0 at 5layer	57%
Detectivity 4layer	$4/87 \times 10^9$
Detectivity 5layer	$7/99 \times 10^9$
% increasing of detectivity at 5layer	39%

To calculate percent can be written [12]:

$$\text{Percentage} = \frac{A2 - A1}{A2} \times 100 \quad \text{if} \quad (A2 > A1) \tag{8}$$

In this work, we reduce the dark current to improve the performance of the photodetector at high temperature (300k) without using the cooling system. To do this, we put a "n" type impurity layer of $In_{1-x}Al_xSb$ material, which has a high band gap, with a thickness of 25nm in the middle of the n+-π regions. This layer is placed to prevent the arrival of n-area carriers who want to enter the active region and cause dark noise. This layer acts as a barrier, like a dam, against the entry of leakage currents into the active region. To reduce further the dark current, we introduced a "p" type impurity layer of $In_{l-x}Ga_xSb$ material with a thickness of 25nm between π-p+. The presence of this layer prevents the arrival of minority carriers in the area of p into the active region, which significantly reduces the dark current in the structure.

4. CONCLUSION

In this paper, we introduced a five-layer infrared photodetector with an InSb / $In_{1-x}Al_xSb$ / InSb / $In_{1-x}Ga_xSb$ / InSb inorganic structure to reduce dark current and increase the precision. Simulation of structure and examination of optical and electrical characteristics was done by Silvaco atlas software. The results showed that inserting the $In_{1-x}Al_xSb$ loop band with x=0.1 between n+-π and $In_{1-x}Ga_xSb$ with x=0.8 between the p+-π region would reduce the effective of dark current and increase resistance and detachment, causing The desired performance of the detector is at room temperature. Our proposed scheme, at T=300k and λ=5μm, has a detectivity of 7.99×10^9 $cmHz^{1/2}/w$, which has found a significant increase.

REFERENCE

[1] A.Rogalski, and K.Chrzanowski, *Infrared devices and techniques*, OPTOELECTRONICS REVIEW 10(2), 111–136, 2002.

[2] E. Michel, and M. Razeghi, *Recent advances in sb-based materials for uncooled infrared photodetectors*, OPTO-ELECTRONIC REVIEW 6(1), 11-23, 1998.

[3] A. Rogalski, *New material systems for third generation inferared photodetectors*, OPTO-ELECTRONICS REVIEW 16(4), 458–482, 2008.

[4] Xin Tang, Guang fu Wu and King Wai Chiu Lai, *Plasmon resonance enhanced colloidal HgSe quantum dot filterless narrowband photodetectors for mid-wave infrared*, Journal of Materials Chemistry C, 2017

[5] Vincenzo Pusino, Chengzhi Xie, Ata Khalid, Member IEEE, Matthew J. Steer, Marc Sorel, Iain G. Thayne, and David R. S. Cumming, Fellow, IEEE, *InSb Photodiodes for Monolithic Active Focal Plane Arrays on GaAs Substrates*, IEEE TRANSACTIONS ON ELECTRON DEVICES, VOL. 63, NO. 8, AUGUST 2016

[6] Mingsheng Long, Anyuan Gao, Peng Wang, Hui Xia, Claudia Ott, Chen Pan, Yajun Fu, Erfu Liu, Xiaoshuang Chen, Wei Lu, Tom Nilges, Jianbin Xu, Xiaomu Wang, Weida Hu, Feng Miao, *Room temperature high-detectivity mid-infrared photodetectors based on black arsenic phosphorus*, SCIENCE ADVANCES RESEARCH ARTICLE, 3: e1700589, 2017

[7] BO WEN JIA, Kian Hua Tan, Wan Khai Loke, Satrio Wicaksono, Kwang Hong Lee, and Soon Fatt Yoon, *Monolithic Integration of InSb Photodetector on Silicon for Mid-Infrared Silicon Photonics*, ACS Photonics, DOI: 10.1021/acsphotonics.7b01546, 2018

[8] Sajjad Khalili, Mohammad Danaie, *Interface analysis of indium antimonide and passive layer in infrared detector and presenting a new structure to improve dark current*, Superlattices and Microstructures, DOI: 10.1016/j.spmi.2018.01.011, S0749-6036(17)32210-3, 2018

[9] Muhammad Shafa, Haining Ji, Lei Gao, Peng Yu, Qinghua Ding, Zhihua Zhou, Handong Li, Xiaobin Niu, Jiang Wu, Zhiming M. Wang, *Mid-infrared photodetectors based on InSb micro/nanostructures grown on low-cost mica substrates*, Materials Letters, DOI: http://dx.doi.org/10.1016/j.matlet.2016.01.063, S0167-577X(16)30065-9, 2016

[10] Chee Leong Tan and Hooman Mohseni, *Emerging technologies for high performance infrared detectors*, Nanophotonics, https://doi.org/10.1515/nanoph-2017-0061,2017

[11] Kun Zhang, Yilun Wang, Weifeng Jin, Xin Fang, Yi Wan, Yinfeng Zhang, Jingzhi Han and Lun Dai, *High-Quality InSb Nanocrystals: Synthesis and Application in Graphene Based Near-Infrared Photodetector*, journal is © The Royal Society of Chemistry View Article Online, DOI: 10.1039/C6RA00503A, 2016

[12] Bringhurst, R. *The Elements of Typographic Style*, 2nd ed. Point Roberts, WA: Hartley and Marks, p. 282, 1997.

[13] A. Rogalski, *Heterostructure infrared photodiodes*, semiconductor physics, Quantum Electronic & Optoelectronics, 3(2), 111-120, 2000.

[14] E. Sijerčić, K. Mueller, and B. Pejčinovic, *Simulation of InSb devices using drift–diffusion equations*, Solid-State Electronics, 49, 1414–1421, 2005.

[15] A. Tevke, C. Besikci, C. V. Hoof, and G. Borghs, *InSb Infrared p-i-n Photodtectors Grown on GaAs Coated Si Substrates by Molecular Beam Epitaxy*, Solid-State Electronics, 42(6), 1039-1044, 1998.

[16] Ghatei Khiabani Azar, H., Rasouli Saghai, H. *Manipulating frequency-dependent diffraction, the linewidth, center frequency and coupling efficiency using periodic corrugations*. Opt Quant Electron, 48: 464.1-12, 2016.

[17] T. Ashley, C. T. Elliott, and A. M. White, *Non-equilibrium devices for infrared detection*, SPIE, 572, Infrared Technology XI, 1985.

[18] A. Piotrowski, P. Madejczyk, W. Gawron, K. Kłos, J. Pawluczyk, M. Grudzień, J. Piotrowski, and A. Rogalski, *MOCVD HgCdTe heterostructures for uncooled infrared Photodetectors*, Quantum Sensing and Nanophotonic Devices II, SPIE, 5732, 273-284, 2005.

[19] M. Nadimi and A. Sadr, *Computer Modeling of MWIR Homojunction Photodetector based on Indium Antimonide*, Advanced Materials Research, 383-390, 6806-6810, 2012.

[20] P. Chakrabarti, A. Krier, and A. F. Morgan, *Double-heterojunction photodetector for mid infrared applications: theoretical model and experimental results*, Society of Photo-Optical Instrumentation Engineers, 42(9), 2614–2623, 2003.

[21] R. K. Lal, M. Jain, S. Gupta, and P. Chakrabarti, *An analytical model of a double-heterostructure mid-infrared photodetector*, Infrared Physics & Technology 44, 125–132, 2003.

[22] T. Ashley, A. B. Dean, C. T. Elliott, A. D. Johnson, G. J. Pryce, A. M. White, and C. R. Whitehouse, *A heterojunction minority carrier barrier for lnSb devices*, Semicond. Sci. Technol. 8, 5386-5389, 1993.

[23] M. Nadimi, and A. Sadr, *Simulation of High Operating Temperature Mid-Infrared Photodetector Based on Indium Antimonide*, Middle-East Journal of Scientific Research, 13(11), 1510-1514, 2013.

[24] J. E. Bowers, and Y. G. Wey, *High-Speed Photodetectors*, Department of Electrical and Computer Engineering University of California, handbook of optic, Chapter 17, 1995.

[25] I. Bhattacharya, *Design and Modeling of Very High-Efficiency Multijunction Solar Cells*, Florida State University Libraries, Summer Semester, 2013.

[26] H. PAGE, The Intrinsic Carrier Dynamics of InGaAs/AIGaAs Single Quantum Well, Strained-Layer, Semiconductor Lasers, PhD. Thesis, Surrey University, 1998.

[27] R. Penumaka, B. Tiwari, I. Bhattacharya, and S. Foo, *Indium Gallium Antimonide a better bottom subcell layer in III-V multijunction solar cells*, Photovoltaic Specialist Conference (PVSC), IEEE 42nd, 1-5, 2015.

[28] M. Nadimi, and A. Sadr, *Modeling and Simulation of High Operating Temperature MWIR Photo Detector Based on Mercury Cadmium Telluride*, International Journal of Computer and Electrical Engineering, 3(4), 597-599, 2011.

[29] P. K. Maurya, and P. Chakrabarti, *Modeling and simulation of heterojunction photovoltaic detector based on InAs$_{0.15}$Sb$_{0.85}$ for free space optical communication*, Journal of Materials Science: Materials in Electronics, 20, 359-362, 2009.

[30] Hamid Faezinia, Mahdi Zavvari, *Quantum modeling of light absorption in graphene based photo-transistors*, Journal of Optoelectronical Nanostructures, Winter 2017 / Vol. 2, No. 1

[31] Khadijeh Hemmati, Esmaiel Saievar-Iranizad, Amir Bayat, *Investigation of hydrothermal process time on the size of carbon micro- and nano-spheres*, Journal of Optoelectronical Nanostructures Spring 2017 / Vol. 2, No. 2

[32] Arash Rezaei, Bahram Azizollah-Ganji, Morteza Gholipour, *Effects of the Channel Length on the Nanoscale Field Effect Diode Performance*, Journal of Optoelectronical Nanostructures, Spring 2018 / Vol. 3, No. 2

[33] Alireza Keshavarz, Zahra Abbasi, *Spatial soliton pairs in an unbiased photovoltaic-photorefractive crystal circuit*, Journal of Optoelectronical Nanostructures, Spring 2016 / Vol. 1, No.1

[34] Hamid Faezinia, Mahdi Zavvari, *Quantum modeling of light absorption in graphene based photo-transistors*, Journal of Optoelectronical Nanostructures, Winter 2017 / Vol. 2, No. 1

[35] Abdolkarim Afroozeh, Seyed Ebrahim Pourmand, *Telepathic Communication Generation using Nano Fiber Ring*, Journal of Optoelectronical Nanostructures, Winter 2018 / Vol. 3, No. 1

[36] Sayed Mohammad Sadegh Hashemi Nassab, Mohsen Imanieh, Abbas Kamaly, *The Effect of Doping and the Thickness of the Layers on CIGS Solar Cell Efficiency*, The Quarterly Journal of Optoelectronical Nanostructures, Spring 2016 / Vol. 1, No.1